International Journal of Bioelectromagnetism *www.ijbem.org*
Vol. 10, No. 4, pp. 261-268, 2008

EEG and Cerebral Blood Flow in Newborns during Quiet Sleep

Botero Rosas, D.A.[1,2], Infantosi, A.F.C.[1], Simpson, D.M.[3], Maldonado Arango, M.I.[2]

1. Biomedical Engeniering Program, Federal University of Rio de Janeiro, Rio de Janeiro, Brazil, Tel (21)2562-8576, Fax (21)2562-8591
2. La Sabana University, Medicine Faculty, Bogotá, Colombia Tel (571)8615555 Ext.2604
3. Institute of Sound and Vibration Research, University of Southampton, Southampton, SO17 1BJ, UK

Correspondence: La Sabana University, Medicine Faculty , Bogotá, Colombia, Phone (571)8615555 Ext.2604

e-mail: danybotero@hotmail.com

Abstract. *Cerebral blood flow (CBF) alterations in the newborns (NB) can lead to brain damage by a decrease in the supply of oxygen and glucose. Aiming at contributing to an understanding of the mechanisms involved, the association between the EEG (right front-temporal derivation) and Doppler velocimetry of the middle cerebral artery from term NB has been investigated. These signals were simultaneously collected from 20 NB and then epochs during quiet sleep (Tracé Alternant, TA, and High Voltage Slow, HVS) were selected. EEG power in theta band (Pthet, 4-8 Hz), was estimated each second. For CBF, obtained from velocimetry, the average velocity (V) was extracted for each heart cycle. To investigate the association in the time (cross correlation function - CCF) and frequency domains (magnitude square coherence - MSC) signal processing techniques were developed that can deal with interruptions in the data (missing samples). During TA, the CCF between Pthet and V resulted in a maximum value around -5 s (Pthet leading V) in 85% of the NBs with $p \leq 0.05$ (significance was tested by Monte Carlo simulations). The maximum of the MSC occurred around 0.10 Hz in 92 % of the NB ($p \leq 0.05$). These findings indicate association between the neuronal activity and CBF during TA. The high coherence could be interpreted as TA influencing CBF or another physiologic variable influencing both the CBF and the neuronal activity.*

Keywords: Cerebral blood flow control, Neonatal EEG, Coherence, Cross-correlation, Autoregulation

1. Introduction

Metabolic activity of the brain requires a constant supply of oxygen, and an increased demand generally leads to increased cerebral blood flow. This control system involves neurogenic, metabolic, myogenic and endothelial mechanisms [Rosengarten et al. 2001; Kuschinsky, 1996] but is still poorly understood. Its dysfunction has however been linked to serious neurological conditions in newborn babies, including ventricular hemorrhage and hypoxic-ischemic encephalopathy [Sándor et al., 2002; Borch et al., 1998; Johansson, 1996; Altman et al., 1987].

Since the 70s, an association between neuronal activity (NA), observed by electroencephalography (EEG), and cerebral blood flow (CBF) measured with $_{133}$Xe, has been suggested [Oishi and Mochizuky 1998, Pryds and Edwards 1996]. However, the CBF measurements possible with this technique are a limitated in the temporal resolution. More recently, transcranial Doppler ultrasound has allowed cerebral blood flow velocity (CBFV) to be monitored non-invasively at very high temporal resolution. This technique allows the study of the relationship between NA and the CBF in physiological conditions such as the sleep-awake cycle, responses to sensory stimuli, and pathological states such as seizures [Kotajima et al. 2005; Panerai et al. 1996].

The current paper provides further evidence of the relationship between CBFV and spontaneous NA in term neonates. In previous work [Simpson et al. 2001, 2005] we described techniques to analyze the relationship between EEG and CBFV signals in recordings that are interrupted by blocks of missing samples. Such gaps in recorded signals are a common feature of recordings carried out in the clinic, and most conventional signal processing techniques cannot be applied in their analysis. We

now provide results from a larger sample of NB than in the previous publications, and study two different patterns of EEG activity.

2. Material and Methods

The Ethics Committee of the Fernandes Figueira Institute (Brazil) approved this study and written informed parental consent was obtained. Twenty full-term NB (gestational age 37-41 weeks) were recruited in the neonatal unit of the Institute during the first week after birth. These NB had normal neurological exams and Apgar ≥ 8 at the first and fifth minute after birth.

2.1 Acquisition and noise-free segments selection

Generally following feeding and with the NB asleep, polisomnography (obtained with the Nihon Kohden, EEG-5414K with standard filter settings of 0.5 to 70 Hz) was carried out, with EEG signals (10 lead montage, International 10-20 System, modified for newborns), electrooculogram (EOG), EMG (sub-mentalis) and ECG (derivation D1) being acquired. The EEG derivation F4-T4 was digitalized and simultaneously the Doppler signal was collected from the right middle cerebral artery (MCA) using a 9.56 MHz continuous wave system (Parks Electronics Lab. 806FC, modified by the Leicester Royal Infirmary, UK). The Doppler maximum frequency envelope was estimated to provide CBFV. Both the CBFV and the EEG signal were sampled at a frequency of 200 Hz. All the polysomnographic signals were also recorded on paper for visual analysis by experienced clinical staff, who determined the awake-sleep stages. Segments of EEG showing quiet sleep (QS), i.e., *tracé alternant* (TA) and high voltage slow (HVS) patterns in the EEG, free of excessive noise or artifact, were thus identified and labeled.

2.2 Extracting the *Pthet* parameter from the EEG

The F4-T4 derivation was chosen because it overlies the cortical region irrigated by the MCA. The digitalized EEG signal during TA and HVS was low-pass filtered (Butterworth, 14th order, 35 Hz cut-off, applied bi-directionally) and the power in Theta frequency band (*Pthet* = 4-8 Hz) was calculated using an FFT (Fast Fourier Transform) in overlapped windows of 1s [Simpson et al. 2001, 2005]. The resulting time-series was low-pass filtered and resampled at 1 Hz. The samples of *Pthet* referring to noise intervals were marked as missing samples, as illustrated in Fig. 1.

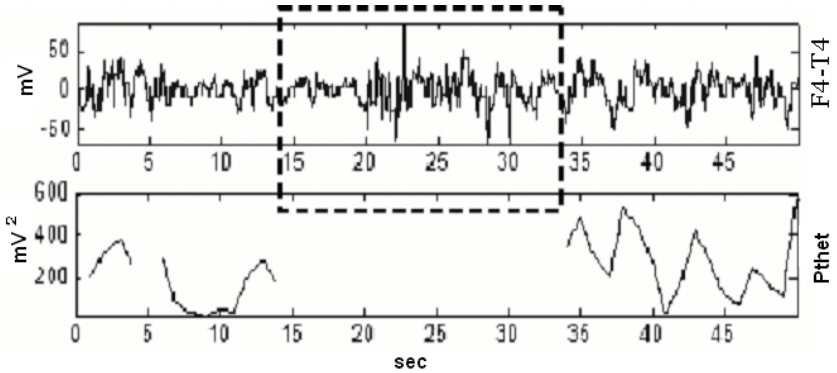

Figure 1. EEG epoch with artifact (frame) and the respective Pthet time series. The gap between 14 and 34 seconds corresponds data that is treated as missing.

2.3 Extracting the mean of CBFV parameter

The CBFV signal was also low-pass filtered (Butterworth, 8th order, 20 Hz cut-off, applied bidirectionally). Spurious peaks were automatically removed using Panerai's algorithm [Panerai et al. 1993] and further peaks were eliminated manually by linear interpolation; periods with artifacts were marked as missing data as in Figure 1, which corresponded to a 0-68% of total duration signals. Evans's algorithm [Evans, 1988] was then applied to detect the up-stroke of each heart-beat, and hence determine the mean CBFV (denoted by *V*) for each cardiac beat. Since the samples in *V* are not

equidistant, cubic spline interpolation with sample spacing of 0.2 s (i.e. a sampling frequency of 5 Hz) was carried out. This was then low-pass filtered (0.5 Hz) and resampled at 1 Hz, to match that of *Pthet*. Figure 2 shows an example of a noisy epoch of CBFV taken from one NB, together with *V*. The data near 5 s and between approximately 14 and 34 s are marked as missing samples.

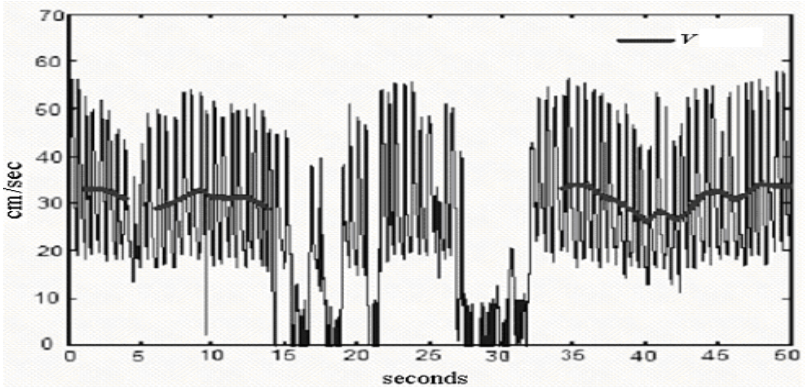

Figure 2. CBFV signal with artifact and the corresponding time series V (bold line). The gap in V near 5 s and between 14 and 34 seconds corresponds to missing data.

2.4 Estimating the Cross Correlation Function with Missing Data

For the time-series *Pthet[i]* and *V[i]* (each of length *N* samples), the Cross Correlation Function (CCF) is estimated as [Brockwell and Davis, 1987]:

$$\hat{CCF}_{Pthet,V}[l] = \frac{\hat{R}_{Pthet,V}[l]}{\sqrt{\hat{R}_{V,V}[0] * \hat{R}_{Pthet,Pthet}[0]}} \tag{1}$$

$$\hat{R}_{Pthet,V}[l] = \frac{1}{N-l} \cdot \sum_{i=0}^{N-l-1} [V[i] - \bar{V}].[Pthet[i+l] - \bar{Pthet}] \tag{2}$$

$$\hat{R}_{V,V}[0] = \frac{1}{N-l} \cdot \sum_{i=0}^{N-l-1} [V[i] - \bar{V}]^2 \tag{3}$$

$$\hat{R}_{Pthet,Pthet}[0] = \frac{1}{N-l} \cdot \sum_{i=0}^{N-l-1} [Pthet[i+l] - \bar{Pthet}]^2 \tag{4}$$

where l is the lag (in samples), $\hat{R}$ represents the estimated auto- and cross-correlations and N-l correspond to the total number of samples used to obtain the estimate of the correlation at each lag, when there are no gaps in the data. When there are missing samples, the number of valid terms in the sums is reduced and the denominator is also diminished accordingly, thus providing an unbiased estimate of the correlations [Simpson *et al.* 2001]. Monte Carlo simulations (surrogate data based on the original *Pthet* and *V* time series) were used to test the statistical significance of the estimated peak value in the cross-correlation functions over lags in the range ±25s [Simpson *et al.* 2001].

2.5 Estimating the Power Spectral Density and Coherence

The coherence may be interpreted as giving the cross-correlation between two signals, selectively by frequency. Thus if two signals are closely correlated only over a narrow range of frequencies, the coherence would show a peak at that frequency. In such signals the cross-correlation function as defined in section 2.4 may not indicate any correlation between the signals, as it merges the results across all frequencies. Coherence may thus be a more sensitive tool for detecting dependence between *Pthet* and *V* at different frequencies. Coherence is based on spectral analysis, as described next.

The power spectral density (PSD) of *Pthet* and *V* were calculated by applying the FFT to the autocorrelation functions, as shown in Eq. 5 and 6:

$$\hat{R}_{Pthet,Pthet}[l] = \frac{1}{N-l} \cdot \sum_{i=0}^{N-l-1} [Pthet[i] - \bar{Pthet}].[Pthet[i+l] - \bar{Pthet}] \tag{5}$$

$$\hat{R}_{V,V}[l] = \frac{1}{N-l} \cdot \sum_{i=0}^{N-l-1} [V[i] - \bar{V}].[V[i+l] - \bar{V}] \quad (6)$$

Again, missing samples lead to a smaller number of terms in the sums, and unbiased estimates are obtained by reducing the denominator correspondingly.

If a NB had more than one QS segment with the same EEG pattern, the mean PSD was calculated from all segments. The median PSD of *Pthet*, denoted as *mPthet*, was calculated using all individual PSDs obtained from the same QS pattern. Similar approach was used to calculate the median PSD of *V*.

The magnitude square of the coherence (MSC) between *Pthet* and *V* was estimated according to Eq.7:

$$\hat{MSC}(f) = \frac{|\hat{P}_{V,P_{thet}}(f)|^2}{\hat{P}_{V,V}(f).\hat{P}_{P_{thet},P_{thet}}(f)} \quad (7)$$

where $\hat{P}_{V,V}(f)$ and $\hat{P}_{Pthet,Pthet}(f)$ are the estimated PSDs of *V* and *Pthet*, respectively, and $\hat{P}_{V,Pthet}(f)$ is the estimate cross spectrum at the frequencies (f). These spectral estimates were all obtained by applying the FFT to the corresponding auto- and cross-correlation functions, as described above. A procedure similar to that described for *mPthet* was employed to calculate the median of the MSC estimate (*m*MSC). The statistical significance of the maximum value of the MSC estimate within a frequency band between 0.06 and 0.2Hz was again tested using the Monte Carlo simulation, as described in a previous work [Simpson *et al.* 2005]. This frequency band was chosen because Zhang et al. demonstrate that at frequencies between 0.07 and 0.3 Hz changes in velocity are linearly related to the changes in pressure [Zhang et al. 1998]

3. Results

The median cross correlation (mCCF) between *Pthet* and *V* for TA and HVS EEG patterns is shown in Fig. 3 (dotted line), together with the results for each subject (solid lines). A total of 13 subjects had one or more epochs of TA that could be analyzed and 10 provided results for HVS. When more than one epoch was available for a subject (see Table 1), the average result for that subject was plotted. During TA the highest value in mCCF was 0.24 at -5s, indicating that changes in CBFV followed those in neuronal activity (NA) with a lag of 5 s. While the peak correlation is quite low, there is a consistent pattern, with the peak observed in most subjects. During HVS, a similar pattern is observed in mCCF, again with a peak at -5s, however the maximum mCCF is lower and there is more scatter between subjects.

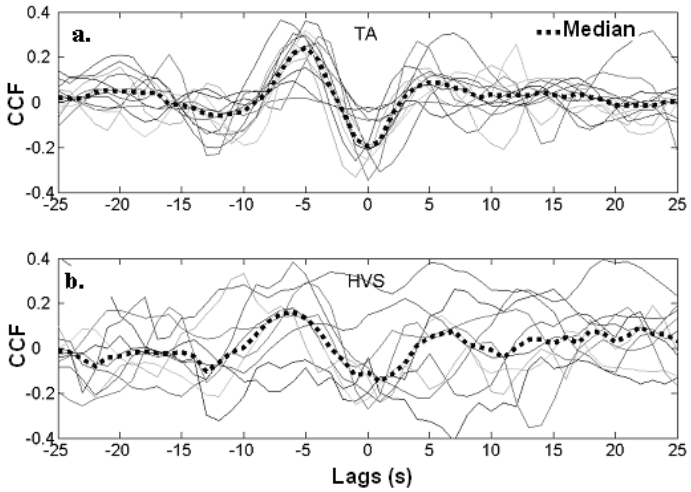

Figure 3. The cross correlation functions of 13 NB during TA and 10 NB during HVS are shown as thin solid lines, and their respective medians as dotted lines.

The statistical significance of peak cross-correlation for each recording is given in Table 1. It may be observed that during TA, significant correlation ($p \leq 0.05$) is found in 13 of the 17 recordings, from of 11 of the 13 subjects (85%). During HVS, 4 of the 10 subjects (40%) gave significant results, with a further 2 being borderline ($p=0.06$). The median PSD for *Pthet* and *V* are shown in Fig. 4 for both TA

and HVS. During TA, the energy of *Pthet* is concentrated around of 0.1 Hz, as may be expected from the approximately 10 s cycle of high and low EEG activity during this EEG activity. During HVS, the energy in *Pthet* is more uniformly distributed between 0.08 and 0.2 Hz. For *V*, power is concentrated at lower frequencies, with similar results for TA and HVS.

Table 1. Peak values of the cross correlation function, the lag at which this occurs and its statistical significance. Results are shown for TA (left) and HVS (right).

	$\hat{r}$ between *Pthe*t and *V* (TA)			$\hat{r}$ between *Pthet* and *V* (HVS)		
NB/Epoch	*P*	*Maximum* $\hat{r}$	*Lag (s)*	*p*	*Maximum* $\hat{r}$	*Lag (s)*
1/1	0.34	0.033	-7	===	====	===
1/2	0.11	0.164	-6	===	====	===
2/1	0.34	0.018	-6	===	====	===
3/1	0.00	0.362	-7	===	====	===
4/1	0.05	0.280	-6	===	====	===
4/2	0.00	0.265	-7	===	====	===
5/1	0.00	0.304	-6	===	====	===
6/1	0.01	0.318	-5	===	====	===
7/1	0.00	0.253	-5	===	====	===
7/2	0.01	0.274	-4	===	====	===
8/1	0.00	0.153	-5	===	====	===
8/2	===	====	===	0.00	0.293	-5
9/1	0.01	0.290	-4	===	====	===
9/2	===	====	===	0.06	0.341	-3
10/1	0.00	0.297	-5	===	====	===
11/1	===	====	===	0.03	0.332	-10
11/2	0.01	0.194	-5	===	====	===
12/1	0.00	0.479	-5	===	====	===
12/2	0.06	0.249	-4	===	====	===
13/1	0.01	0.243	-5	===	====	===
14/1	===	====	===	0.06	0.149	0
15/1	===	====	===	0.90	0.175	-6
16/1	===	====	===	0.68	-0.043	0
17/1	===	====	===	0.64	-0.052	-5
18/1	===	====	===	0.08	0.149	-4
19/1	===	====	===	0.05	0.181	-6
20/1	===	====	===	0.00	0.384	-6

Furthermore, when the *mV* during TA is compared with its corresponding in HVS at 0.1Hz kept equal (Fig. 4).

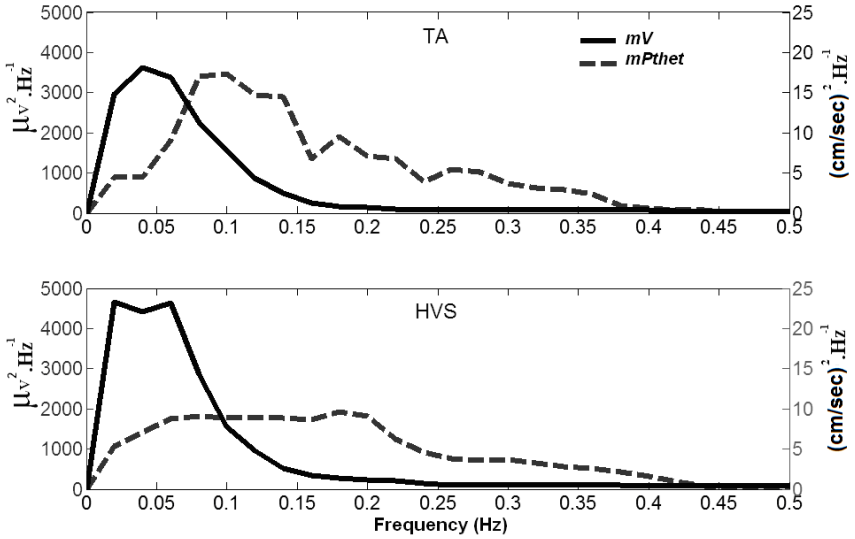

Figure 4. Median of the PSDS for Pthet (dotted line) and V (continuous line) for TA (top) and HVS (bottom).

The maximum of the MSC occurred in the range from 0.08 to 0.12 Hz during TA (Fig. 5 and Table 2) and reached statistical significance ($p<0.05$) for 12 of the 13 NBs. During HVS the maximum

coherence was also in this frequency range, and significant in 5 of the 10 NBs. It may be noted that the peak MSC is found to occur at similar frequencies for both TA and HVS.

Table 2. Peak value of MSC and the frequency at which this occurs, together with the p-value of that peak. The results for TA (left) and HVS (right) are shown.

	MSC *Pthet* and *V* (TA)			**MSC *Pthet* and *V* (HVS)**		
NB/Epoch	**Max MSC**	**Max.Freq MSC (Hz)**	***p-fmax***	**Max MSC**	**Max.Freq MSC (Hz)**	***p-fmax***
1/1	0.182	0.16	0.07	--------	--------	--------
1/2	0.310	0.10	0.04	--------	--------	--------
2/1	0.228	0.10	0.04	--------	--------	--------
3/1	0.412	0.08	0.00	--------	--------	--------
4/1	0.798	0.14	0.01	--------	--------	--------
4/2	0.525	0.08	0.00	--------	--------	--------
5/1	0.556	0.12	0.00	--------	--------	--------
6/1	0.512	0.12	0.02	--------	--------	--------
7/1	0.425	0.08	0.00	--------	--------	--------
7/2	0.477	0.12	0.00	--------	--------	--------
8/1	0.397	0.12	0.00	--------	--------	--------
8/2	-------	--------	-------	0.500	0.10	0.00
9/1	0.491	0.10	0.01	--------	--------	--------
9/2	-------	--------	-------	0.001	0.08	0.56
10/1	0.340	0.10	0.00	--------	--------	--------
11/1	-------	--------	--------	0.383	0.20	0.19
11/2	0.427	0.10	0.00	--------	--------	--------
12/1	0.238	0.08	0.11	--------	--------	--------
12/2	0.342	0.10	0.20	--------	--------	--------
13/1	0.458	0.10	0.00	--------	--------	--------
14/1	-------	--------	-------	0.173	0.12	0.01
15/1	-------	--------	-------	0.338	0.10	0.01
16/1	-------	--------	-------	0.176	0.08	0.03
17/1	-------	--------	-------	0.249	0.08	0.35
18/1	-------	--------	-------	0.229	0.18	0.17
19/1	-------	--------	-------	0.321	0.10	0.02
20/1	-------	--------	-------	0.137	0.08	0.18

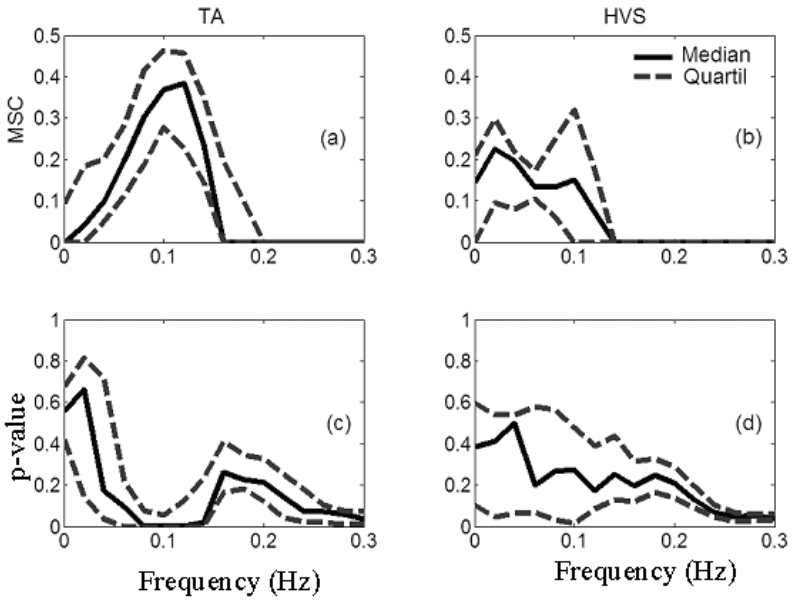

Figure 5. Median MSC (solid line) and Quartiles (dashed lines) between Pthet and V during (a) TA and (b) HVS. The respective p-values are shown in (c) and (d).

4. Discussion

In earlier work we observed statistically significant cross correlation between NA in the theta band and CBF during TA [Simpson *et al.* 2001], and NA changes were noted to occur five seconds before of CBF variations. This has now been confirmed on the expanded sample of NB included in this work. In addition, now we also show that similar (average) cross-correlation is obtained during HVS, again with a delay of approximately 5 s. Though the peak CCF values are lower and only 4 out of 10 cases gave $p<0.05$, overall this can still be considered statistically significant (binomial distribution, $p<0.05\%$). The similarity in results provides further evidence that spontaneous fluctuations in NA (as reflected in the EEG) regulate CBF in healthy term neonates. These findings may be interpreted as indicating that neurological mechanisms have a less evident role in the control of CBF during HVS, than during TA.

An alternative explanation is that due to the less pronounced slow variations in *Pthet* during HVS, the CBFV is less tightly linked with NA. It is well established that CBF is also under the control of many factors and mechanisms [Mraovicth, 1996, Udomphorn et al. 2007] including the spontaneous variations in blood pressure, arterial CO2 and O2, and intracranial and venous pressure, as well as spontaneous vasomotion. Furthermore, non-linear and time- and frequency-varying effects may further contribute to the reduced correlation. The neurological mechanism may operate by controlling the CBF with time delays near to five seconds – as observed in previous work [Simpson *et al.* 2001]. Ursino *et al.* [1998] also suggest that pressure-dependent mechanisms (neurogenic or myogenic), exhibit dynamics shorter than 10 seconds.

A number of studies have described increases in CBF while the individual progresses from sleep to waking, which show an increase in NA. [Kotajima *et al.* 2005, Iadecola *et al. 1997*, Schwartz, 2007]. In this work (Figure 4), the PSD of *Pthet* shows an increase in the energy when the NB pass from TA to HVS in agreement with the cited works. We observed that the energy in frequencies of 0.02 to 0.07 Hz (band of very low frequencies strongly diminish when the NBs pass from TA to HVS probably due to a major participation of mechanisms that are not relate with neurological control of the CBF, [Zhang et al. 1998]. During TA also was observed that the energy of the neurons in theta rhythm mainly arise in frequencies around of 0.1 Hz when the NB enters into TA, probably, this is due to increments of the neurological control, to maintain the CBF when others mechanism diminish their influence on the CBF control. Ferrari *et al.* [1996] and Zhang *et al.* [2002] suggest that neurological mechanism may be responsible for the control of CBF in frequencies between 0.07 and 0.3Hz. Other observation is that during HVS the energy of the neurons oscillating in theta is distributed more uniformly when compared with TA, since during deep sleep the neurological control seem to be concentrated around of the frequency 0.1Hz.

Our findings related to the coherence function indicate a significant association between the neuronal activity in theta rhythm and the CBF about 0.1 Hz during TA. During HVS this association is present as well, but with fewer cases reaching statistical significance. Additionally during this last pattern a second peak in the VLF (<0.07 Hz) is observed, which probably means an increased influence by other mechanisms of control that should be different to the neurogenic regulation. While the NB transit by the HVS pattern, probably various mechanisms work simultaneously regulating the CBF, then, the neurogenic control should diminish their influence on the CBF at this time.

The work described here clearly indicates that spontaneous variations in CBFV are associated with spontaneous variations in EEG activity in the theta band of neonates during quiet sleep. While it seems most plausible that this reflects a physiological response of cerebral arterioles to changes in neuronal activity, other mechanisms may be active. It is possible that some (as yet unknown) mechanism is driving both the EEG and CBF changes. Alternatively, changes in arterial blood pressure may be driving the observed changes in CBFV. This possibility should be addressed in future work in which a wider range of physiological signal are recorded simultaneously.

ACKNOWLEDGMENT

To the Brazilian Agencies CAPES – Ministry of Education and CNPq – Ministry of Science and Technology for the financial support and to the Fernandes Figueira Institute (FIOCRUZ - Ministry of Health/Brazil) for providing the infrastructure support. Finally, to Dr. L. Fan and Prof. D.H. Evans (Leicester University – UK) for providing the Doppler acquisition system.

References

Borch K, Greisen G. Blood Flow Distribution in the Normal Human Preterm Brain. *Pediatric Research,* 43(1): 28-33, 1998

Brockwell P. J., Davis R. A, Time series: theory and methods, Springer-Verlag, New York, 1987

Evans D.H. A Pulse-Foot-Seeking algorithm for Doppler ultrasound waveform, *Clinical physics and physiological measurement.* 9: 267-271, 1988

Ferrari F., Kelsall W.R., Rennie J.M., Evans D.H., The Relationship bettween Cerebral Blood Flow Velocity Fluctuations and Sleep State in Normal Newborns, *Pediatric Research,* 35(1): 50-54, 1993

Iadecola C., Yang G., Ebner T.J., Chen G., Local and Propagated Vascular Response Evoked by Focal Synaptic Activity in Cerebellar Cortex. *Journal of Neurophysiology,* 78: 651-659, 1997

Johansson B.B, Clinical Implications (1): Stroke, Subarachnoid Haemorrhage and Epilepsy in Neurophysiological Basis of Cerebral Blood Flow Control: An Introduction. Sima Mraovitch and Richard Sercombe Editors. John Libbey, London,1996, 359-372.

Kotajima F., Meadows G. E., Morrell M.J., Corfield D.R. Cerebral blood flow changes associated with fluctuations in alpha and theta rhythm during sleep onset in humans. *The Journal of Physiology*, 568(1): 305-313, 2005

Kuschinsky W., Regulation of cerebral blood flow: an overview in Neurophysiological Basis of Cerebral Blood Flow Control: An Introduction. Sima Mraovitch and Richard Sercombe Editors. John Libbey, London, 1996, 245-262.

Mraovich S., Neurogenic Regulation of Cerebral Blood Flow: Intrinsec Neural Control. Sima Mraovitch and Richard Sercombe Editors. John Libbey, London, 1996, 323-354.

Oishi M, Mochizuki Y., Correlation between contingent negative variation and regional cerebral blood flow. *Clinical Electroencephalography*. 29(3): 124-127, 1998

Panerai R. B., Coughtrey H., Rennie J. M. A model of the instantaneous pressure-velocity relationships of the neonatal cerebral circulation. *Physiological Measurement,* 14(4): 411-418, 1993

Pryds O., Edwards A.D., Cerebral blood flow in the newborn infant, *Archives of Disease in Childhood - Fetal and Neonatal Edition*, 74(1): 63-69, 1996

Rosengarten B, Huwendiek O, Kaps M. Neurovascular Coupling and Cerebral Autoregulation can be Described in Terms of a Control System. *Ultrasound in Medicine & Biology*, 27(2): 189-193, 2001

Sandor P, Benyó Z., Erdös B, Lacza Z, Komjáti K. The Roy-Sherrington hypothesis: facts and surmises. *International Congress Series* 1235: 325-335, 2002

Schwartz T.H., Neurovascular Coupling And Epilepsy: Hemodynamic Markers For Localizing And Predicting Seizure Onset, *Current Review in Clinical Science*, 7(4):91-94, 2007

Simpson D.M., Botero-Rosas D.A., Infantosi A.F.C., Estimation of coherence between blood flow and spontaneous EEG activity in neonates, *IEEE Transactions on Biomedical Engineering*, 52(5):852-858, 2005

Simpson D.M., Infantosi A.F.C., Botero-Rosas D.A., Estimation and significance testing of cross-correlation between cerebral blood flow velocity and background electro-encephalograph activity in signals with missing samples, *Medical and Biological Engineering and Computing,* 39: 428-433. 2001

Udomphorn Y., Armstead W.M., Vavilala M.S., Cerebral Blood Flow and Autoregulation After Pediatric Traumatic Brain Injury. *Pediatric Neurology*, 38:225-234, 2008

Ursino M., Lodi C.A., Interaction among autoregulation, CO2 reactivity, and intracranial pressure: a mathematical model, American Journal of Physiology, 274(5 Pt 2): H1715-H1728, 1998

Zhang R., Zuckerman J.H., Iwasaki K., Wilson T., Crandall C.G., Levine B.D., Autonomic Neural Control of Dynamic Cerebral Autoregulation in Humans, *Circulation* 106: 1814-1820, 2002

Zhang R., Zuckerman J.H., Giller C.A., Levine B.D., Transfer Function Analysis of Dynamic Cerebral Autorregulation in Humans, American Journal of Physiology *43*: H233-H241, 1998